

Engineering Surface Segregation of Perovskite Oxide through Wet Exsolution for CO Catalytic Oxidation

Zhen Li^{a,b}, Xiyang Wang^{b*}, Xinbo Li^c, Minli Zeng^a, Carl Redshaw^d, Rui Cao^e, Ritimukta Sarangi^e, Changmin Hou^c, Zuolong Chen^b, Wenhua Zhang^f, Nannan Wang^{a*}, Xiaofeng Wu^{c*}, Yanqiu Zhu^a, and Yimin A. Wu^{b*}

Z. L., M. Z., Prof. N. W., Prof. Y. Z.

^a Guangxi Institute Fullerene Technology (GIFT), State Key Laboratory of Featured Metal Resources and Advanced Materials, School of Resources, Environment and Materials, Guangxi University, Nanning, 530004, P. R. China

Z. L., Dr. X. W., Dr. Z. C., Prof. Y. A. W.

^b Department of Mechanical and Mechatronics Engineering, Waterloo Institute for Nanotechnology, Materials Interface Foundry, University of Waterloo, Waterloo, Ontario N2L 3G1, Canada

X. L., Prof. C. H., Dr. X. W.

^c State Key Laboratory of Inorganic Synthesis and Preparative Chemistry, College of Chemistry, Jilin University, Changchun, 130012, P. R. China

Prof. C. R.

^d Plastics Collaboratory, Department of Chemistry, University of Hull, Hull HU6 7RX, U.K. Dr. R. C., Dr. R. S.

^e Stanford Synchrotron Radiation Light source SLAC National Accelerator Laboratory Menlo Park California 94025, USA

^f National Synchrotron Radiation Laboratory, University of Science and Technology of China, Hefei 230029, Anhui, China

‡ These authors contributed equally.

E-mail: xiyang.wang@uwaterloo.ca; wangnannan@gxu.edu.cn; wuxf@jlu.edu.cn

Keywords: perovskite oxides, surface segregation, wet exsolution, surface/interface electronic structure, CO oxidation

© 2022. This manuscript version is made available under the CC-BY-NC-ND 4.0 license: <http://creativecommons.org/licenses/by-nc-nd/4.0/>

Abstract

Cation segregation occurring near the surface or interfaces of solid catalysts plays an important role in catalytic reactions. Unfortunately, the native surface of perovskite oxides is dominated by passivated A-site segregation, which severely hampers the catalytic activity and durability of the system. To address this issue, herein, we present a wet exsolution method to reconstruct surface segregation in perovskite cobalt oxide. Under reduction etching treatment of glycol solution, inert surface Sr segregation is transformed into active Co_3O_4 segregation. By varying the reaction time, we can achieve differing coverage of the active Co_3O_4 segregation on the perovskite oxide surface. This study reveals that CO oxidation activity exhibits a volcano-shaped dependence on the coverage of Co_3O_4 segregation at the surface of a perovskite cobalt oxide. Furthermore, we find that a suitable coverage of Co_3O_4 segregation can dramatically improve the catalytic activity of the perovskite catalyst by enhancing interface interactions. Co K-edge, Co L-edge, and O K-edge X-ray absorption spectra confirm that the synergistic effect optimizes the covalence of the metal-oxygen bond at the surface and interface. This work not only contributes to the design and development of perovskite-type catalysts, but also provides important insight into the relationship between surface segregation and catalytic activity.

1. Introduction

The emissions of carbon monoxide from lime kilns, synthetic ammonia plants, petrochemical plants, and vehicle exhaust have a significant negative impact on the global environment.¹⁻³ In order to eliminate emitted noxious carbon monoxide gas, it is essential to develop catalysts that are both affordable and highly efficient.⁴ Among the various catalysts, perovskite-type catalysts have attracted wide attention because of their flexible tunable structure, low cost, and enhanced thermostability.⁵⁻⁹ In a typical perovskite structure of formula ABO_3 , the larger A-site cation

located at the edge of the structure is an alkaline, alkaline-earth, or lanthanide cation, and the smaller B-site cation located at the center of the metal-oxygen octahedron is a 3d, 4d, or 5d transition metal.^{5,10} Usually, the key role of the A-site cation is to stabilize the crystal structure of the perovskite material, while the B-site cation is an important active center during the catalytic process.^{5, 8, 11} However, the native surface of a perovskite oxide is dominated by inactive A-site cations (surface segregation), resulting in a severe underestimate of the true catalytic performance.¹²⁻¹⁴ Therefore, ways in which to engineer the surface composition and structure of a perovskite oxide in order to improve overall performance and durability is a valuable research topic. Progress in this area will promote the development of perovskite-type catalysts in future practical applications.

Over the past decade, many strategies have been developed in order to activate surface segregation or to suppress the enrichment of A-site cations during catalysis.¹⁵⁻¹⁷ In brief, current research on the tuning of surface segregation of perovskite oxides tends to focus on the following three points: i) acid etching treatment¹⁸⁻²⁰, ii) surface decoration^{16,21-23}, and iii) *in-situ* exsolution of the B-site metal cation^{9, 15, 24-27}. In acid etching technology, excess surface A-site cation segregation can be removed partly by using certain inorganic acids. After acid etching treatment, the SrO/BaO segregations at the surface of SrTi_{1-x}Fe_xO_{3.8} and GdBaCo₂O_{6.8} exhibit a distinct decrease, which prominently reduces the polarization resistance during electrochemical reactions.^{19, 28} In our previous work, we have also obtained the Mn-enriched perovskite La_{0.5}Sr_{0.5}MnO₃ by etching treatment using dilute nitric acid, and this led ultimately to excellent CO oxidation activity.²⁹ These results indicate that reducing the coverage of surface A-site segregation can increase the surface active sites available and improve the capability for electron transfer. A surface modification strategy can be envisaged that appropriately decorates the secondary phase material at the surface of the perovskite oxide. Many modification materials have been studied to improve the performance and durability of perovskite oxides via

interface interactions, which include Co_3O_4 , HfO_2 , Nb_2O_5 , TiO_2 , ZrO_2 , LaSrCoO_4 , Sr segregation, and so on.^{16,21,22,30} The special interface interactions not only enhance the activation and dissociation of molecular oxygen, but also suppress further enrichment of A-site cation segregation during the catalytic process. Different from these two methods, for *in-situ* exsolution technology, the B-site metal can be *in-situ* precipitated at the surface of the parent perovskite via external forces (e.g. heat, electricity, and pressure).^{12, 25, 27, 31} Based on this principle, Pt, Ni, Co, Fe, and Pd metals or metal alloy nanoparticles are *in-situ* grown at the surface of the perovskite oxide via high-temperature annealing under a reducing atmosphere.^{9, 14, 24, 32} These *in-situ* exsolved perovskite catalysts display excellent catalytic performances and durability because of increased surface-active sites and a strong metal-oxide interface. To obtain BO_x segregation at the surface of perovskite oxides, a wet exsolution method has also been developed to selectively dissolve the A cation. Based on this, the perovskite LaMnO_3 can be processed into active $\text{MnO}_2/\text{LaMnO}_3$ by surface reconstruction under acidic conditions.³³ Our previous work also demonstrates that the perovskite $\text{La}_{0.3}\text{Sr}_{0.7}\text{CoO}_3$ can be reconstructed into the $\text{Co}_3\text{O}_4/\text{La}_{0.3}\text{Sr}_{0.7}\text{CoO}_3$ composite material via treatment with ethylene glycol and high-temperature annealing.¹² Therefore, a wet treatment can be used to control surface BO_x segregation of perovskite cobalt oxides by optimizing the reaction conditions. Additionally, it is imperative to offer insights into the relationship between surface coverage for BO_x segregation and catalytic performance.

Herein, we prepare perovskite cobalt oxides with a different surface coverage of Co_3O_4 segregation via the wet exsolution method. Use of an inductively coupled plasma emission spectrometer (ICP) and an energy dispersive spectrometer (EDS) demonstrate that the dissolution of the Sr ion and surface reconstruction in the perovskite cobalt oxide manufacture, *i.e.*, the surface Co_3O_4 segregation and the surface coverage can be controlled by tuning the etching time of the glycol. The CO oxidation activity shows a volcano-shaped dependence on the coverage of surface Co_3O_4 segregation. X-ray absorption (XAS) and X-ray photoelectron

(XPS) spectroscopies, *in-situ* DRIFTS, and electron microscopy further clarify that the appropriate Co_3O_4 segregation displays the best interface interactions with the parent perovskite and significantly optimizes the covalence of the cobalt-oxygen bond.

2. Result and discussion

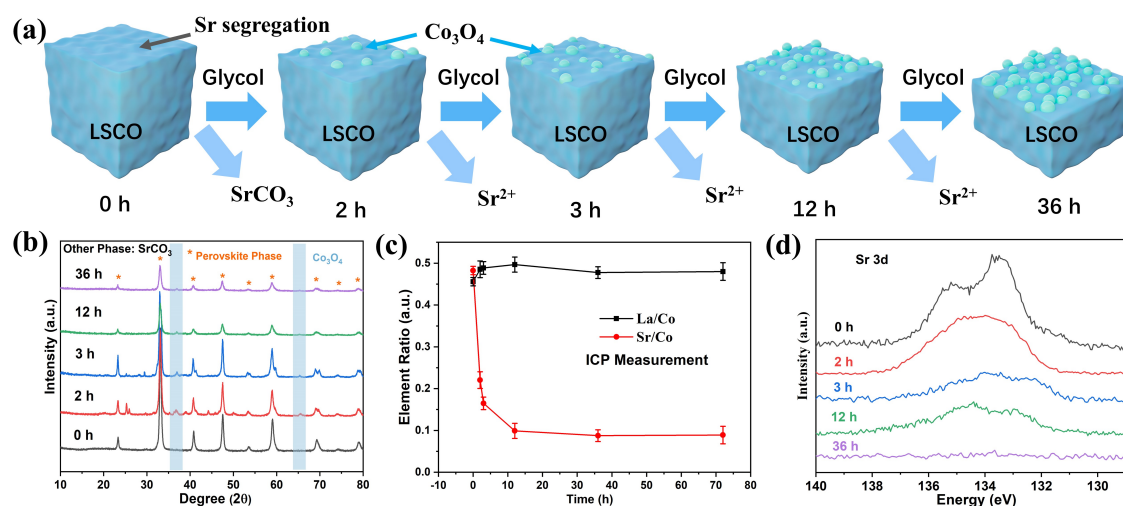


Figure 1. Composition and structure of the perovskite catalysts. (a) Illustration of the evolution route of surface Co_3O_4 segregation in the perovskite cobalt oxide via wet exsolution. (b) X-ray diffraction (XRD) patterns, (c) ICP analysis, and (d) Sr 3d XPS spectrum of LSCO-0 h, LSCO-2 h, LSCO-3 h, LSCO-12 h, and LSCO-36 h.

The perovskite $\text{La}_{0.5}\text{Sr}_{0.5}\text{CoO}_{3-\delta}$ (LSCO) was first prepared using the sol-gel method and the synthetic details are shown in the experimental section in the Supporting Information.³⁴ It is well-known that the native surface of the perovskite $\text{La}_{0.5}\text{Sr}_{0.5}\text{CoO}_{3-\delta}$ is dominated by passivated Sr segregation.^{17, 30} To increase the number of surface active sites and improve the catalytic performance of the perovskite LSCO, an *in-situ* wet exsolution strategy was developed to tune the surface composition and structure, where glycol was applied as the etching and reducing agent to remove Sr ions in the lattice and to achieve the reconstruction of the surface structure (Figure 1a). In this process, perovskite LSCO is mixed with thoroughly with glycol solution,

and the system is transferred to a Teflon autoclave reactor and subjected to a solvothermal reaction at 120 °C for 2 h, 3 h, 12 h, and 36 h, respectively. As shown in **Figure 1a**, as the reaction time was prolonged, the Sr ions in the perovskite lattice are gradually removed and the surface coverage of reconstructed Co_3O_4 segregation also shows a distinct increase.

To investigate the crystal structure of these materials, XRD patterns are measured. **Figure 1b** shows that the main phase of LSCO-0 h, LSCO-2 h, LSCO-3 h, LSCO-12 h, and LSCO-36 h is a cubic $Pm\bar{3}m$ perovskite structure. After the etching treatment with glycol, the crystal phase of Co_3O_4 gradually emerges. Moreover, we find that perovskite LSCO-2 h also reveals an increase in the amount of SrCO_3 impurity present after a two-hour processing period, however the SrCO_3 impurity dissolves and disappears as the reaction time increases. According to this XRD result, the above conclusion seems reasonable. Furthermore, the element contents of La, Sr, and Co in these catalysts were measured using an ICP instrument. As shown in **Figure 1c**, the ratio of La content to Co content does not reveal much change, but the content of Sr reveals undergoes a severe decrease. After treatment for 12 h, the Sr content in perovskite LSCO remains largely unchanged. Therefore, we infer that the key role of the glycol is to selectively dissolve Sr atoms in perovskite lattice and it has little effect on the La and Co atoms. XPS as a surface-sensitive tool was also employed to analyze the surface composition of these materials. The Sr 3d XPS spectrum in **Figure 1d** reveals that when extending the reaction time, the surface Sr content in perovskite LSCO decreases progressively and there is no Sr element at the surface of LSCO-36 h. The La 3d XPS spectrum in **Figure S1** reveals that surface La element undergoes a weak increase after the etching treatment, stemming from the reduction of Sr. The Sr 3d XPS results obtained from these samples are consistent with the ICP, XRD, and theoretic predictions regarding surface reconstruction in perovskite oxides.

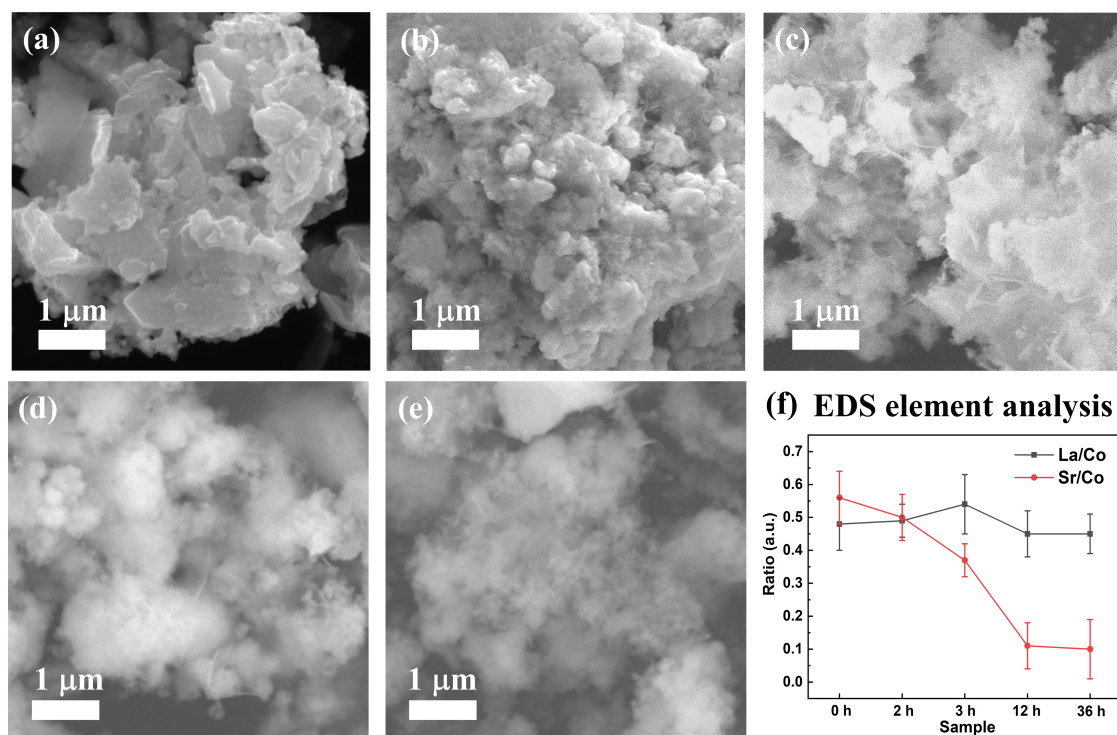


Figure 2. Surface morphology. SEM images of (a) LSCO-0 h, (b) LSCO-2 h, (c) LSCO-3 h, (d) LSCO-12 h, and (e) LSCO-36 h, (f) element ratio of LSCO-0 h, LSCO-2 h, LSCO-3 h, LSCO-12 h, and LSCO-36 h via EDS measurement.

To observe the influence of surface segregation on the surface morphology, SEM images of LSCO-0 h, LSCO-2 h, LSCO-3 h, LSCO-12 h, and LSCO-36 h were measured, respectively. **Figure 2 a-e** shows that the pristine perovskite LSCO-0 h is a large bulky material. When treated with glycol, its surface becomes rough and the thickness also becomes thinner. Furthermore, the corresponding EDS of these materials was recorded to analyze the element content. **Figure 2f** shows that there are relatively few changes to the amount of La element present in the perovskite catalysts after treatment, but there is a marked decline in the Sr element concentration, which confirms the above experimental results. To probe the composition and structure of these samples, TEM and HRTEM images were recorded, respectively. **Figures S2-S6** show that on increasing the reaction time from 0 h, 2 h, 3 h, 12 h, to 36 h, the perovskite materials gradually get thinner and there is a meaningful increase in the specific surface area (BET). The BET values at 0 h, 2 h, 3 h, 12 h, and 36 h are 3.65 m²/g, 7.99 m²/g, 10.93 m²/g,

16.53 m²/g, and 20.49 m²/g, respectively. **Figure 3** shows that the pristine perovskite LSCO is a pure phase structure without obvious defects, and as a result of the glycol treatment, the crystal phase of Co₃O₄ in the composite perovskite materials increases with the treatment time. This result indicates that the surface coverage of Co₃O₄ segregation in perovskite LSCO is improved by the etching treatment. Furthermore, the enlarged perovskite lattice image in **Figure 3c** reveals that in the perovskite structure there exist some defects, vacancies, and distortions due to the removal of the Sr ions.

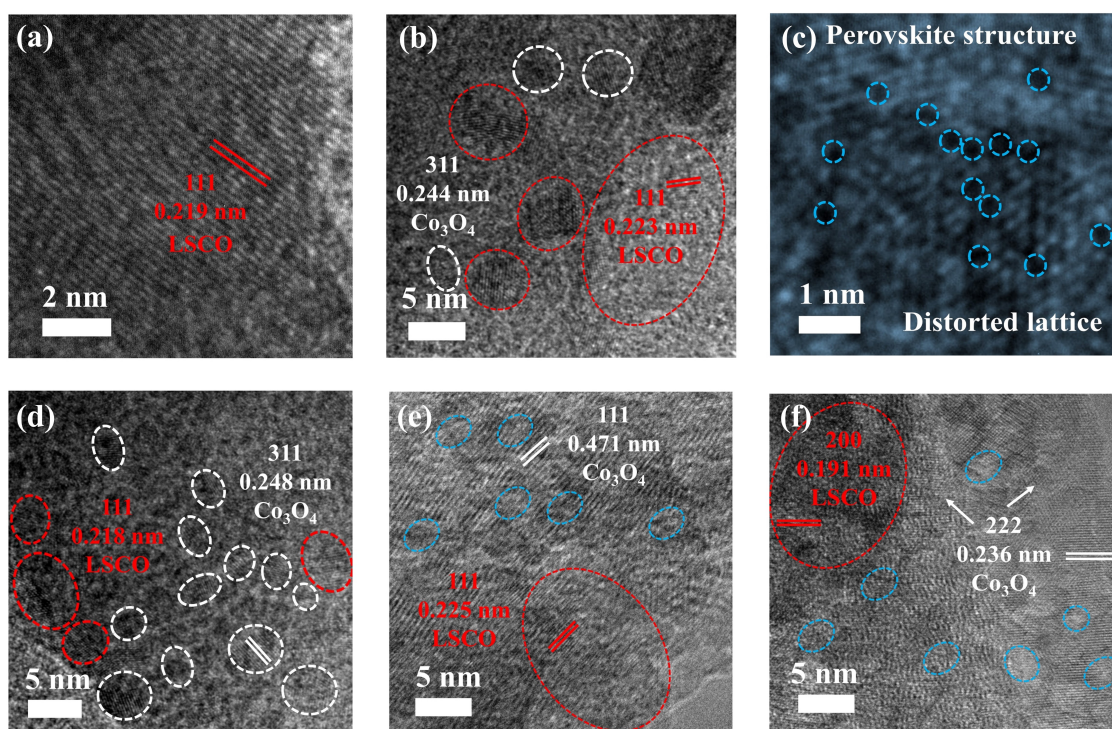


Figure 3. Crystal phase structure and surface segregation. HRTEM images of (a) LSCO-0 h, (b) LSCO-2 h, (c) enlarge perovskite structure in LSCO-2 h, (d) LSCO-3 h, (e) LSCO-12 h, and (f) LSCO-36 h. The red circle represents the perovskite material, the white circle represents Co₃O₄ segregation, the blue circle represents some defect structure, whilst most of the materials in e and f are Co₃O₄ segregation.

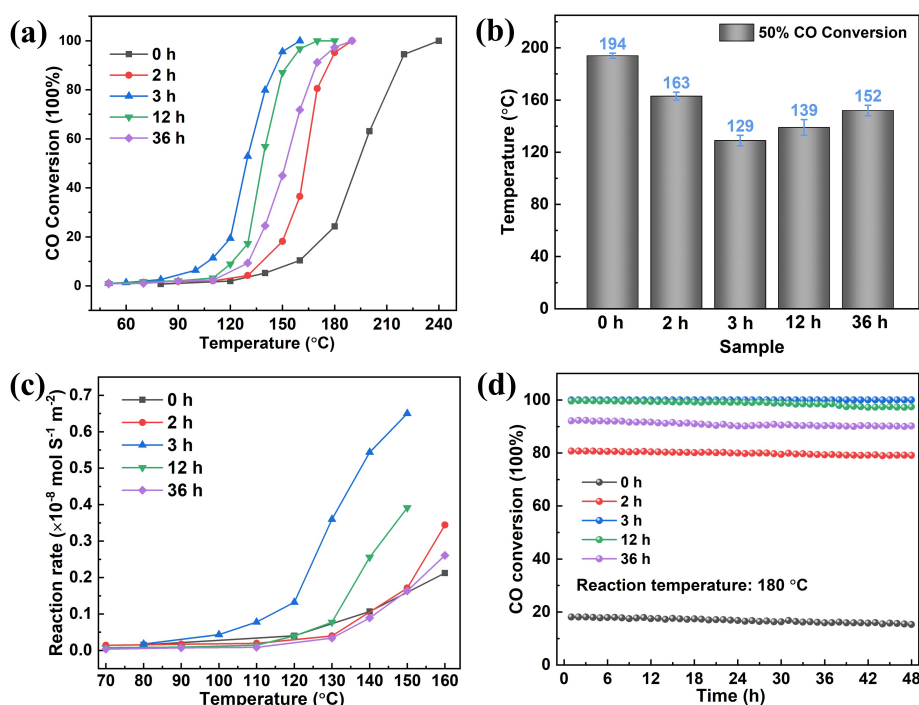


Figure 4. Catalytic oxidation activity of perovskite catalysts. (a) CO catalytic oxidation curves, (b) $T_{50\%}$ temperature, (c) reaction rate normalized by specific surface area, and (d) operational durability at 180 °C of LSCO-0 h, LSCO-2 h, LSCO-3 h, LSCO-12 h, and LSCO-36 h.

To investigate the influence of surface segregation in the perovskite oxides on catalytic activity, the CO oxidation activity of these samples was measured. **Figure 4a** shows that the CO catalytic oxidation activity exhibits a volcano-shaped dependence on the coverage of Co_3O_4 segregation at the surface of the perovskite cobalt oxide, and the perovskite LSCO-3 h with suitable Co_3O_4 segregation possesses the best catalytic performance. The $T_{50\%}$ conversion temperatures for LSCO-0 h, LSCO-2 h, LSCO-3 h, LSCO-12 h, and LSCO-36 are 194 °C, 163 °C, 129 °C, 139 °C, and 152 °C, respectively (**Figure 4b**). To better study the intrinsic catalytic activity, the reaction rates normalized by the specific surface area of these samples were also calculated. As shown in **Figure 4c**, the perovskite LSCO-3 h exhibits the highest reaction rate, whilst the second highest is the LSCO-12 h system. While LSCO-0 h, LSCO-2 h, and LSCO-36 h have similar catalytic reaction rates, although LSCO-36 h has the largest specific surface area. What's more, **Figure 4d** shows that perovskite LSCO-3 h also possesses better stability than the other perovskite catalysts and the durability of the perovskite LSCO-0 h with Sr

segregation is the worst. Based on these catalytic results, we conclude that the native surface Sr segregation in perovskite oxides can passivate the surface sites and thereby decrease the catalytic activity, while the coverage of the decorated surface Co_3O_4 segregation should be neither too much nor too little.

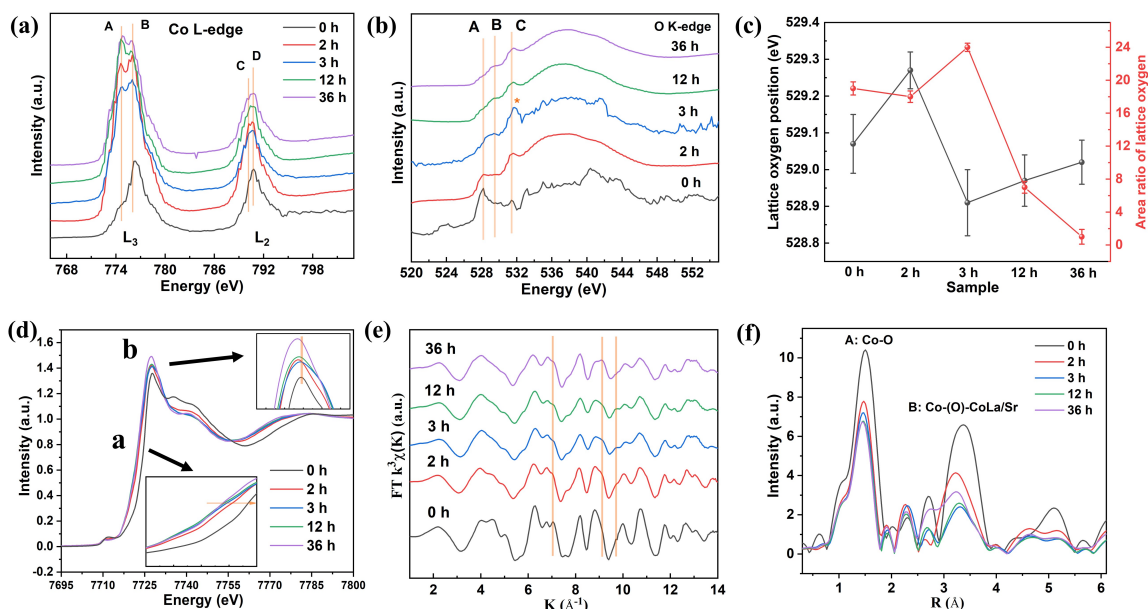


Figure 5. Electronic structure. (a) Co L-edge XANES spectrum, (b) O K-edge XANES spectrum, (c) lattice oxygen, (d) Co K-edge XANES spectrum, (e) K-space Fourier-transformed FT ($k^3\chi(k)$) of Co K-edge EXAFS, and (f) R-space Fourier-transformed FT ($k^3\chi(k)$) of Co K-edge EXAFS of LSCO-0 h, LSCO-2 h, LSCO-3 h, LSCO-12 h, and LSCO-36 h.

To elucidate the relationship between the Co_3O_4 segregation, electronic structure, and catalytic activity, the Co L-edge and O K-edge XANES spectra, together with the XPS and Co K-edge XAFS spectra were recorded, respectively. The Co L-edge XANES spectrum in **Figure 5a** reveals that the Co atom in LSCO-0 h has the highest average oxidation state due to a high energy shift in peak B.³⁴ After increasing the surface Co_3O_4 segregation, two adsorption peaks (A and B) were observed in the Co L-edge XANES spectrum. We find that the intensity ratio of the peak A to peak B exhibits only a weak improvement, which demonstrates a decrease of the oxidation state in Co atom with the increase of Co_3O_4 content. The Co 2p XPS spectrum in **Figure S7** confirms the result relating to the oxidation state of the Co element in the Co L-edge

XAS spectrum. The O K-edge XANES spectrum was used to study the covalency of the Co-O bonds at the surface/interface of the perovskite oxides.^{12, 34} As displayed in **Figure 5b**, the ratio of peak A to peak B intensity reveals a gradual decrease, and the average peak position for both peaks A and B shifts to high energy. This illustrates that the synergistic effect of the interface and Co₃O₄ segregation improves the covalence of the Co-O bonds in these composite materials. Furthermore, we observe that peak C in LSCO-3 h has a high energy position compared with the other samples, which suggests that the surface oxygen species in LSCO-3 h is more active than in the other samples. The O 1s XPS spectrum was also recorded to study the surface electronic structure with that of LSCO-0 h, LSCO-2 h, LSCO-3 h, LSCO-12 h, and LSCO-36 h fitted into adsorption oxygen and lattice oxygen (**Figures S8-S13**). As displayed in **Figure 5c**, the peak positions and peak areas of the lattice oxygen are plotted as a line chart. LSCO-3 h possesses a more active surface lattice oxygen than the other samples, which indicates that the excessive surface segregation increases the amount of surface adsorbed oxygen species, but reduces the exposure to oxygen active sites. Furthermore, the energy position of the lattice oxygen in LSCO-3 h is the lowest, which stems from the strong interface interactions and high covalence of the Co-O bond in the perovskite LSCO-3 h. Therefore, the presence of appropriate surface Co₃O₄ segregation not only increases the amount of exposed surface-active oxygen sites, but also optimizes the electronic structure at the surface and interface. Finally, the Co K-edge XAFS spectrum of these materials was recorded to analyze the local structure around the Co atom. The Co K-edge XANES spectrum in **Figure 5d** reveals that the X-ray adsorption edge in **region?** and the X-ray adsorption peak in the b region have shifted to low energy, which demonstrates that the average oxidation state of the Co atom in these catalysts decreases gradually with increased glycol reaction time. The K-space Fourier-transformed FT ($k^3\chi(k)$) of the Co K-edge EXAFS in **Figure 5e** indicates that this data has a better signal-noise ratio and that the main phase structure is the same. After treatment with glycol, it was observed that a small amount of Co₃O₄ crystallizes on the perovskite catalysts. The R-space Fourier-

transformed FT ($k^3\chi(k)$) of the Co K-edge EXAFS in **Figure 5f** shows that after removing the Sr ions in the perovskite lattice, the peak intensity in the first shell exhibits a clear decrease, which indicates that the disorder of the Co-O bond is increasing. However, for the second shell involving Co-La/Sr/Co bonds, it was observed that the peak intensity first increases, then decreases, with LSCO-3 h possessing the weakest peak intensity. This disorder in the second shell displays a volcanic dependence on the coverage of Co_3O_4 segregation and the disorder of LSCO-3 h is the highest amongst these perovskite catalysts. These results illustrate that an adequate coverage of surface segregation can optimize the surface electronic structure and improve the catalytic activity.

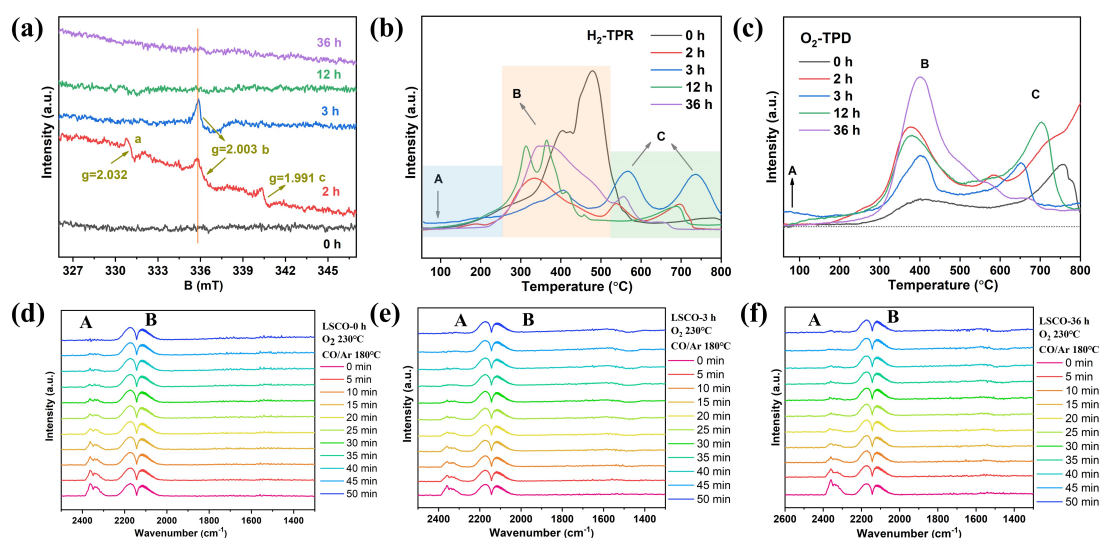


Figure 6. Chemical properties of perovskite catalysts. (a) EPR spectra measured at room temperature under air, (b) H_2 -TPR profile, and (c) O_2 -TPD profile of LSCO-0 h, LSCO-2 h, LSCO-3 h, LSCO-12 h, and LSCO-36 h. *In-situ* DRIFTS of CO adsorption at different times over (d) LSCO-0 h, (e) LSCO-3 h, and (f) LSCO-36 h.

The EPR spectra in **Figure 6a** reveal that for LSCO-3 h, there exists three different EPR signals at g values of 2.032, 2.003, and 1.991, which are considered to be SrO (Surface) related oxygen species, oxygen vacancy, and SrO (bulk) related oxygen species, respectively.^{35, 36} By contrast, LSCO-2 h, LSCO-0 h, LSCO-12 h, and LSCO-36 h do not display any obvious signals

in their EPR spectra. Different from these samples, LSCO-3 h only exhibits a strong EPR signal of $g=2.003$, which is ~ 1.8 times (stronger?) than that of LSCO-2 h. The EPR results indicate that LSCO-3 h possesses more oxygen vacancies and that LSCO-2 h contains more SrO/SrCO₃ segregation. Moreover, when increasing the Co₃O₄ segregations, the amount of oxygen vacancies decreases. The H₂-TPR profile in **Figure 6b** shows that LSCO-3 h has the lowest reduction temperature for the adsorbed surface oxygen species in the A region compared to the other samples. Suitable surface segregations can optimize interface interactions to improve the activity of surface oxygen species. In the B and C regions of the H₂-TPR profile, it was observed that for LSCO-2 h, 3h, 12 h, and 36 h samples there is a lower reduction temperature for Co³⁺/Co⁴⁺ → Co²⁺ and Co²⁺ → Co⁰ compared with LSCO-0 h, which stems from the surface Co₃O₄ segregations.^{5, 8} Furthermore, the O₂-TPD profile shows that LSCO-3 h possesses a lower temperature for the onset peak (A) of the surface oxygen species desorption compared to the other samples.³⁶ When increasing the Co₃O₄ surface segregations, the desorption temperature of the surface lattice oxygen (B) and the bulk lattice oxygen (C) also exhibit an obvious decrease, which indicates that the Co₃O₄ segregations can facilitate the mobility of the lattice oxygen. **Figures S6d-S6f** display the *in-situ* DRIFTS for the CO adsorption at different times over LSCO-0 h, LSCO-3 h, and LSCO-36 h, where peak A is assigned as the absorption of CO₂ and peak B represents the absorption of CO over the solid catalyst.^{36, 37} It was observed that LSCO-3 h possessed a stronger desorption ability than either LSCO-0 h and LSCO-36 h because the signal attenuation for the CO₂ absorption in LSCO-3 h is greater over the same reaction time. The *in-situ* DRIFTS results illustrate that suitable surface Co₃O₄ segregations can promote the desorption of CO₂ and improve the catalytic activity.

3. Conclusion

In summary, we have prepared perovskite cobalt oxides with active surface Co₃O₄ segregation via the wet exsolution method. Variation of the reaction time allowed us to adjust the coverage

of active Co_3O_4 segregation at the surface of perovskite cobalt oxide. This study reveals that CO oxidation activity is strongly dependent on the coverage of segregated Co_3O_4 present at the surface of the perovskite cobalt oxide. Moreover, appropriate Co_3O_4 segregation can optimize the electronic structure at the surface and interface, which involves the covalency of transition metal-oxygen bond, the oxidation state of the metal cations, and the activity of surface sites. Therefore, the CO catalytic oxidation activity of the perovskite cobalt oxide exhibits a volcano-like dependence for the coverage of the Co_3O_4 segregation. This work not only illustrates the correlation between surface segregation, surface/interface electronic structure, and catalytic activity, but also provides a new pathway for the design and control of surface segregation in perovskite oxides.

Author Contributions

The manuscript was written through the contributions of all authors. All authors have approved the final version of the manuscript. ‡These authors contributed equally.

Z.L.: experiment operation, some regular characterizations, and original draft; **X.W.:** material design, data treatment, data analysis, writing-original draft preparation, review, and edition; **B.L.:** partial characterizations for CO oxidation, H_2 -TPR and O_2 -TPD; **M.Z.:** in-situ FTIR and soft XAS measurements; **C.H.:** XPS measurement; **R.C. and R.S.:** XAFS measurement and discuss; **Z.C.:** data discussion and revision; **X.W. and N.W.:** review, edition, revision, supervision, and funding acquisition; **C.R., Z.Y. and W.Y.:** review, editing, revision and some important guidance.

Notes

The authors declare no competing financial interest

Supporting Information

Supporting Information is available from the Wiley Online Library or from the author.

Acknowledgments

The work is supported by the National Natural Science Foundation (51972068 and 21801090), the Natural Science Foundation of Guangxi (2018GXNSFBA138025), and the users with Excellence Program of Hefei Science Center CAS (2020HSC-UE002). Y. A. W thanks the support from the Natural Science and Engineering Research Council (NSERC) of Canada (RGPIN-2020-05903, GECR-2020-00476). CR thanks the EPSRC for an Overseas Travel Grant (EP/R023816/1). The authors thank beamlines MCD-A and MCD-B (Soochow Beamline for Energy Materials) in National Synchrotron Radiation Laboratory (NSRL) for providing beam time. The authors thank BL7-3 in Stanford Synchrotron Radiation Light source (SSRL) for help with characterizations. Z. L. and X. W. contributed equally to this work.

Received: (will be filled in by the editorial staff)

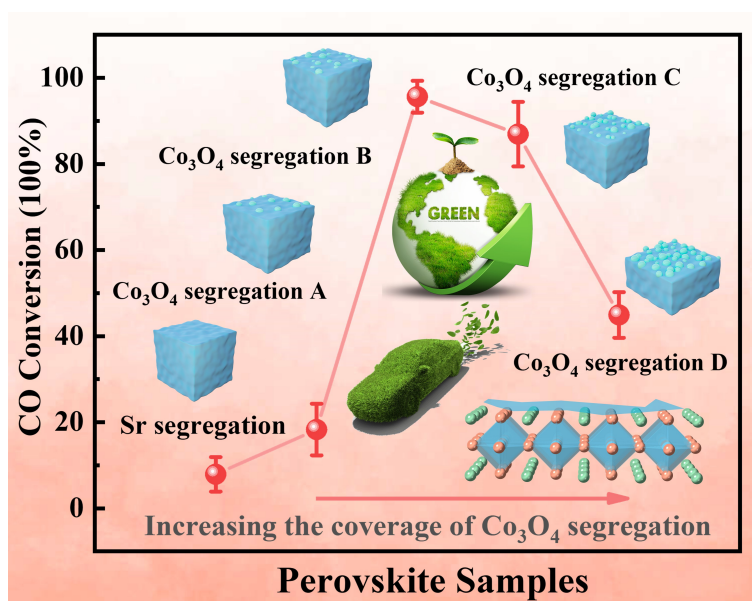
Revised: (will be filled in by the editorial staff)

Published online: (will be filled in by the editorial staff)

References

1. L. Zhang, W. Liu, K. Hou, J. Lin, C. Song, C. Zhou, B. Huang, X. Tong, J. Wang, W. Rhine, Y. Jiao, Z. Wang, R. Ni, M. Liu, L. Zhang, Z. Wang, Y. Wang, X. Li, S. Liu, Y. Wang, *Nat. Commun.* **2019**, *10*, 3741.
2. P. R. F. Cordero, K. Bayly, P. Man Leung, C. Huang, Z. F. Islam, R. B. Schittenhelm, G. M. King, C. Greening, *The ISME Journal* 2019, *13*, 2868;
3. X. Li, L. Jin, H. Kan, *Nature* **2019**, *570*, 437.
4. J. Neugeboren, D. Borodin, H. W. Hahn, J. Altschäffel, A. Kandratenka, D. J. Auerbach, C. T. Campbell, D. Schwarzer, D. J. Harding, A. M. Wodtke, T. N. Kitsopoulos, *Nature* **2018**, *558*, 280.
5. S. Royer, D. Duprez, F. Can, X. Courtois, C. Batiot-Dupeyrat, S. Laassiri, H. Alamdari, *Chem. Rev.* **2014**, *114*, 10292.
6. Y. Zhou, X. Guan, H. Zhou, K. Ramadoss, S. Adam, H. Liu, S. Lee, J. Shi, M. Tsuchiya, D. D. Fong, S. Ramanathan, *Nature* **2016**, *534*, 231.
7. J. Hwang, R. R. Rao, L. Giordano, K. Akkiraju, X. R. Wang, E. J. Crumlin, H. Bluhm, Y. Shao-Horn, *Nat. Catal.* **2021**, *4*, 663.
8. J. Zhu, H. Li, L. Zhong, P. Xiao, X. Xu, X. Yang, Z. Zhao, J. Li, *ACS Catal.* **2014**, *4*, 2917.
9. M. Kothari, Y. Jeon, D. N. Miller, A. E. Pascui, J. Kilmartin, D. Wails, S. Ramos, A. Chadwick, J. T. J. N. C. Irvine, *Nat. Chem.* **2021**, *13*, 677.
10. M. A. Peña, J. L. G. Fierro, *Chemical reviews* **2001**, *101*, 1981.
11. X. Wang, X. Li, X. Chu, R. Cao, J. Qian, Y. Cong, K. Huang, J. Wang, C. Redshaw, R. Sarangi, G. Li, S. Feng, *Adv. Funct. Mater.* **2021**, *31*, 2006439.
12. X. Wang, Z. Pan, X. Chu, K. Huang, Y. Cong, R. Cao, R. Sarangi, L. Li, G. Li, S. Feng, *Angew. Chem. Int. Ed.* **2019**, *58*, 11720.
13. W. Zhang, W. Zheng, *ChemCatChem* **2015**, *7*, 48.
14. Y. Cong, Z. Geng, Q. Zhu, H. Hou, X. Wu, X. Wang, K. Huang, S. Feng, *Angew. Chem. Int. Ed.* **2021**, *60*, 23380.

15. Y. Song, H. Li, M. Xu, G. Yang, W. Wang, R. Ran, W. Zhou, Z. Shao, *Small* **2020**, *16*, 2001859.
16. N. Tsvetkov, Q. Lu, L. Sun, E. J. Crumlin, B. Yildiz, *Nat. Mater.* **2016**, *15*, 1010.
17. B. Koo, K. Kim, J. K. Kim, H. Kwon, J. W. Han, W. Jung, *Joule* **2018**, *2*, 1476.
18. S. Li, Z. Geng, X. Wang, X. Ren, J. Liu, X. Hou, Y. Sun, W. Zhang, K. Huang, S. Feng, *Chem. Commun.* **2020**, *56*, 2602.
19. W. Jung, H. L. Tuller, *Energy Environ. Sci.* **2012**, *5*, 5370.
20. D. Wang, Y. Peng, Q. Yang, S. Xiong, J. Li, J. Crittenden, *Environ. Sci. Technol.* **2018**, *52*, 7443.
21. G. M. Rupp, A. K. Opitz, A. Nanning, A. Limbeck, J. Fleig, *Nat. Mater.* **2017**, *16*, 640.
22. Z. Feng, Y. Yacoby, M. J. Gadre, Y.-L. Lee, W. T. Hong, H. Zhou, M. D. Biegalski, H. M. Christen, S. B. Adler, D. Morgan, Y. Shao-Horn, *J. Phys. Chem. Lett.* **2014**, *5*, 1027.
23. E. Mutoro, E. J. Crumlin, M. D. Biegalski, H. M. Christen, Y. Shao-Horn, *Energy Environ. Sci.* **2011**, *4*, 3689.
24. D. Neagu, T. S. Oh, D. N. Miller, H. Menard, S. M. Bukhari, S. R. Gamble, R. J. Gorte, J. M. Vohs, J. T. Irvine, *Nat. Commun.* **2015**, *6*, 8120.
25. J. H. Myung, D. Neagu, D. N. Miller, J. T. Irvine, *Nature* **2016**, *537*, 528..
26. L. Yang, Y. Li, Y. Sun, W. Wang, Z. Shao, *Energy Environ. Mater.* 2021, doi:10.1002/eem2.12256.
27. D. Neagu, G. Tsekouras, D. N. Miller, H. Menard, J. T. Irvine, *Nat. Chem.* **2013**, *5*, 916.
28. J. Druce, H. Tellez, M. Burriel, M. D. Sharp, L. J. Fawcett, S. N. Cook, D. S. McPhail, T. Ishihara, H. H. Brongersma, J. A. Kilner, *Energy Environ. Sci.* **2014**, *7*, 3593.
29. K. Huang, X. Chu, L. Yuan, W. Feng, X. Wu, X. Wang, S. Feng, *Chem. Commun.* **2014**, *50*, 9200..
30. Y. Li, W. Zhang, Y. Zheng, J. Chen, B. Yu, Y. Chen, M. Liu, *Chem. Soc. Rev.* **2017**, *46*, 6345.
31. O. Kwon, S. Sengodan, K. Kim, G. Kim, H. Y. Jeong, J. Shin, Y.-W. Ju, J. W. Han, G. J. N. c. Kim, *Nat. Commun.* **2017**, *8*, 15967.
32. A. K. Opitz, A. Nanning, V. Vonk, S. Volkov, F. Bertram, H. Summerer, S. Schwarz, A. Steiger-Thirsfeld, J. Bernardi, A. Stierle, J. Fleig, *Nat. Commun.* **2020**, *11*, 4801.
33. W. Si, Y. Wang, S. Zhao, F. Hu, J. Li, *Environ. Sci. Technol.* **2016**, *50*, 4572.
34. X. Wang, K. Huang, L. Yuan, S. Xi, W. Yan, Z. Geng, Y. Cong, Y. Sun, H. Tan, X. Wu, L. Li, S. Feng, *J. Phys. Chem. Lett.* **2018**, *9*, 4146..
35. V. Seeman, A. Lushchik, E. Shablonin, G. Prieditis, D. Gryaznov, A. Platonenko, E. A. Kotomin, A. I. Popov, *Sci. Rep.* **2020**, *10*, 15852.
36. J. Yang, S. Hu, Y. Fang, S. Hoang, L. Li, W. Yang, Z. Liang, J. Wu, J. Hu, W. Xiao, C. Pan, Z. Luo, J. Ding, L. Zhang, Y. Guo, *ACS Catal.* **2019**, *9*, 9751.
37. B. Zheng, T. Gan, S. Shi, J. Wang, W. Zhang, X. Zhou, Y. Zou, W. Yan, G. Liu, *ACS Appl. Mater. Interfaces* **2021**, *13*, 27029.



Here, we present a wet exsolution method to activate the surface segregation of perovskite cobalt oxides. Variation of the reaction time allows us to adjust the coverage of Co_3O_4 segregation. The CO oxidation activity exhibits a volcano-shaped dependence on the coverage of Co_3O_4 segregation on the surface of the perovskite cobalt oxide. Appropriate Co_3O_4 segregation can optimize the surface/interface electronic structure and improve the catalytic performance. This work illustrates the correlation between segregation, surface/interface electronic structure, and catalytic activity and opens up a new pathway for engineering surface segregation in perovskite oxides.